

MODELING SURFACE ROUGHNESS EFFECTS AND EMISSION PROPERTIES OF BULK AND LAYERED METALLIC PHOTOCATHODES*

D. A. Dimitrov, G. I. Bell, Tech-X Corp., Boulder, CO 80303, USA

I. Ben-Zvi, J. Smedley, BNL, Upton, NY 11973, USA

J. Feng, S. Karkare, H. A. Padmore, LBNL, Berkeley, CA 94720, USA

Abstract

The thermal limit of the intrinsic emittance of photocathodes represents an important property to measure experimentally and to understand theoretically. Detailed measurements of intrinsic emittance have become possible in momentatron experiments. Moreover, recent developments in material design have allowed growing photoemissive layers with controlled surface roughness. Although analytical formulations of the effects of roughness have been developed, a full theoretical model and experimental verification are lacking. We aim to bridge this gap by developing realistic models for different materials in the three-dimensional VSim particle-in-cell code. We have recently implemented modeling of electron photo-excitation, transport, and emission from photoemissive layers grown on a substrate. We report results from simulations with these models on electron emission from antimony and gold. We consider effects due to density of states, photoemissive layer thickness, surface roughness and how they affect the spectral response of quantum yield and intrinsic emittance.

INTRODUCTION

Modern developments in design and synthesis of materials have resulted in photocathodes that can deliver high quantum efficiency, operate at visible wavelengths, and are robust enough to work in high electric field gradient photoguns for application to free electron lasers (FEL), advanced X-ray light sources, in dynamic electron microscopy and diffraction. Synthesis, however, often results in roughness, ranging from the nano to the microscale. Thus, the effects on roughness on emittance are of significant importance to understand [1, 2].

MODELING

We use the VSim Particle-in-Cell (PIC) code to simulate electron emission from photocathodes with flat and controlled rough surfaces. We consider parallel ridges, as shown in Fig. 1, since these can be grown experimentally. We have described in detail [3] the models we have implemented to enable such simulations for metallic materials together with the parameters of the rough surfaces ridges that we simulate. Our approach includes electron excitation in response to absorption of photons, charge transport, representation of flat and rough interfaces, modeling emission taking into

account image charge and local field enhancement effects, efficient 3D electrostatic solver for a simulation domain that has sub-domains with different dielectric properties. We applied these models first [3] to study electron emission from antimony with the electron-electron (el-el) scattering mean free path (MFP) calculated from a simple four-parameter model that did not include the effect of temperature.

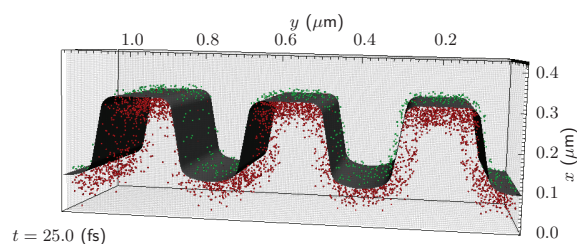


Figure 1: Electrons are loaded (red spheres) due to absorption of photons. Electrons emitted in vacuum (green spheres) drift in applied electric field. The translucent gray surface is the interface between the photocathode and vacuum.

Here, we study quantum yield (QY), the ratio of emitted electrons to absorbed photons, from both Au and Sb and its dependence on cathode roughness, work function variation on the emission surface, and the density of states (DoS). For electron emission from metallic materials, el-el scattering is the most important process to model. Most often, a single el-el scattering event reduces the energy of sufficiently energetic photo-excited electron below the threshold for emission. For the Sb simulations, we used the simple empirical model for the el-el MFP that we implemented initially [3] with the set of parameters that showed good agreement with experimental data on intrinsic emittance. For modeling electron transport in gold, we implemented a higher-fidelity el-el scattering model. It was proposed by Jensen *et al.* [4] and includes the effect of temperature on the MFP. It depends only on one parameter. We also implemented a 3-step model (TSM) [5, 6] for calculation of QY from Au and compare simulation results with it.

RESULTS

We ran simulations with the implemented models for Au and Sb to investigate how surface roughness, variable work function and density of states affect quantum yield and intrinsic emittance. For the simulations with a flat emission surface, we used a uniform work function $\phi = 4.5$ eV for Sb [2] and 4.9 eV for Au [7]. Note, however, that values for the work function of gold have been reported in the range from 4.6 to 5.47 eV depending on emission crystal surface

* We are grateful to the U.S. DoE Office of Basic Energy Sciences for supporting this work under the grant DE-SC0013190.

orientations and types of studies. We have already provided a detailed account [3] of the three-dimensional simulation setup and the rough surface parameters for Sb. We use the same simulation setup and a rough surface interface for the Au simulation here as well. However, we have now developed a new charged particle loader in VSim that enables loading electrons in a photocathode material due to absorption of photons with given energy and absorption length. It can be configured to load electrons over time and as a function of laser intensity. We used the new particle loader for all QY simulation results presented here.

Simple models for the DoS of materials (e.g., a constant DoS or $\sim \sqrt{\mathcal{E}}$ from the free electron model) are often used [6] to investigate QY and intrinsic emittance. Alternatively, optical DoS has been obtained from analysis of photoemission experimental data [7] (for the case of gold). However, simple models for the DoS are not sufficient to explain experimental data as in the case of intrinsic emittance from Sb [2] while using a DoS from band structure calculations showed agreement with the measurements [2, 3]. Thus, similarly to the case of Sb, we incorporated in the Au simulations a DoS extracted from band structure calculations, shown in Fig. 2 (relative to the chemical potential μ). The figure also displays two modified DoS curves that we used to study how changes in the DoS affect QY. Note that the optical DoS [7] for Au shows differences compared to the calculated one [8].

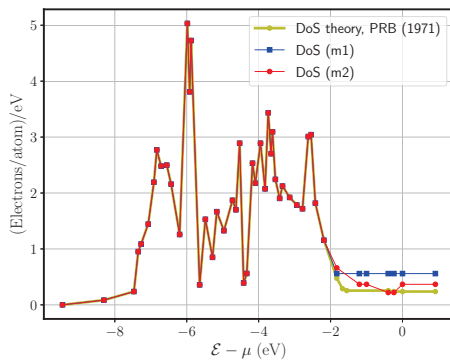


Figure 2: The DoS for Au was extracted from band structure calculations [8]. We also used two modified curves (m1 and m2) to study DoS effects.

For the TSM results, we calculated QY numerically following the approach to derive quantum efficiency given by Dowell *et al.* [6]. This leads to the following equation:

$$QY(\omega) = \frac{\int_{\mu+\phi-\hbar\omega}^{\infty} d\mathcal{E} p(\mathcal{E}, \omega) \int_{\cos\theta_{max}}^1 d(\cos\theta) F_{ee}}{2 \int_{\mu-\hbar\omega}^{\infty} d\mathcal{E} p(\mathcal{E}, \omega)}, \quad (1)$$

where \mathcal{E} is the electron energy in the conduction band from which it is excited to energy $\mathcal{E} + \hbar\omega$ due to absorption of a photon with energy $\hbar\omega$. The function

$$p(\mathcal{E}, \omega) = g(\mathcal{E} + \hbar\omega)(1 - f(\mathcal{E} + \hbar\omega))g(\mathcal{E})f(\mathcal{E})$$

is assumed to be proportional to the probability (per unit energy) for this photo-excitation process [6], $g(\mathcal{E})$ is the electron density of states, ϕ is the work function, $f(\mathcal{E})$ is the Fermi function, θ is the angle between the electron momentum and the emission surface normal. The probability that a photo-excited electron reaches the emission surface without scattering with another electron is

$$F_{ee}(\mathcal{E}, \omega, \cos\theta) = \frac{\lambda_{ee}(\mathcal{E} + \hbar\omega) \cos\theta}{\lambda_{opt}(\omega) + \lambda_{ee}(\mathcal{E} + \hbar\omega) \cos\theta},$$

where $\lambda_{ee}(\mathcal{E})$ is the el-el MFP, $\lambda_{opt}(\omega)$ is the photon absorption length. The cosine of the maximum angle (relative to the emission surface normal) an electron incident on the surface can have and be emitted into vacuum with conservation of transverse momentum is given [6] by $\cos\theta_{max} = \sqrt{(\mu + \phi)/(\mathcal{E} + \hbar\omega)}$.

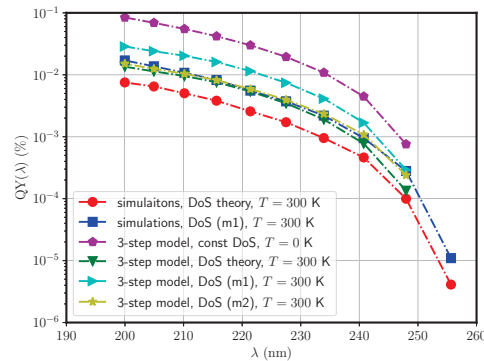


Figure 3: Simulation results and 3-step model calculations on QY from Au indicate the importance of including the gold DoS in these approaches.

The TSM for the QY in Eq. (1) assumes a unity probability of emission for $\mathcal{E} > \mu + \phi$ when $\theta \leq \theta_{max}$ (where ϕ is generally the effective work function including the Schottky barrier lowering [6]) and zero for $\mathcal{E} \leq \mu + \phi$. In the simulations, the emission probability is calculated with the local potential at each attempted electron interface crossing (and along a direction normal to the emission surface) using a transfer matrix method [3]. This takes into account both electron tunneling and over barrier reflection.

We show results on QY from Au from the simulations and different approximations with the TSM in Fig. 3. The range of photon wavelengths is similar to the range used in the Sb emission experiments [2]. The two sets of simulation results show the sensitivity of the QY on small changes in the DoS near the Fermi level. Data on the DoS of Au from different studies [7, 8] show changes of similar magnitude. The simulation results with the modified DoS (m1) show agreement with available QY experimental data [7] while the QY from the simulations with the band structure DoS is lower. Using a constant DoS and the $T = 0$ K Fermi function in the TSM, the approach developed previously [6], we obtain QY that is several times higher than the experimental data and the simulations. The QY from the TSM with the

band structure DoS is much closer to the simulations data (and similarly for the case with the modified DoS) though still somewhat higher. Note also that the QY from the TSM is 0 for $\lambda \geq 253$ nm (not explicitly shown in Fig. 3) since in Eq. (1) the probability of emission is assumed zero for $\mathcal{E} \leq \mu + \phi$. The simulations do not have this restriction and, moreover, initial electron energies are sampled from the tail of the distribution with $\mathcal{E} > \mu$. These results indicate that the actual DoS of Au has to be included in the models and in the simulations in order to obtain results in agreement with experimental data on QY.

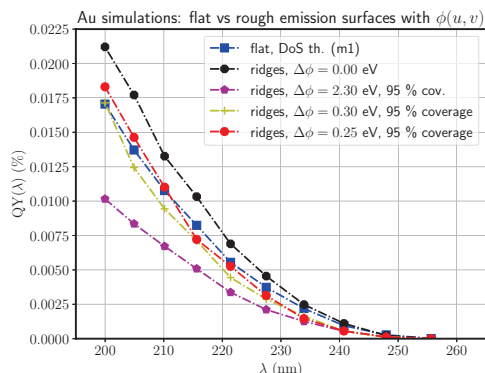


Figure 4: Surface roughness and variable work function effects could lead to a crossover in the QY relative to emission from a flat surface.

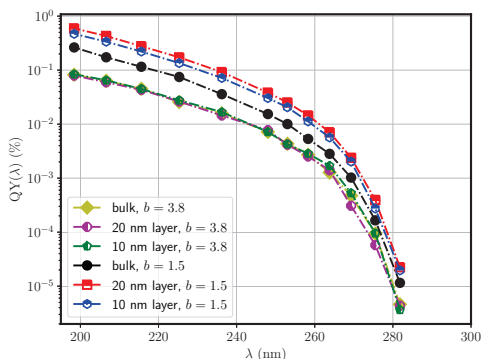


Figure 5: Effects of finite layer width and different el-el MFP on the QY from Sb.

In Fig. 4, we show simulation results on the effect of surface roughness and variable work function on QY from Au. Results on QY from Sb are similar but the QY is higher since Sb has a lower work function. The QY from the ridges surface is somewhat higher than from the flat one since photons absorbed on the sides of the ridges excite electrons effectively closer to the emission surface. Increasing ϕ only on the sides of the ridges (over 95 % of the sides area), reduces emission there. For some value $\Delta\phi$ of the increase, there is a wavelength λ_c where a crossover can be observed: the QY from the rough surface is higher than from the flat one for $\lambda < \lambda_c$ and drops below it for $\lambda > \lambda_c$.

Results on QY from simulations on emission from Sb layers and two different el-el MFPs are shown in Fig. 5. The runs with the el-el scattering model parameter $b = 1.5$ cor-

respond to the longer MFP [3]. The finite layer width affects the QY only for the runs with $b = 1.5$. However, simulations with $b = 3.8$ (shorter MFP) lead to agreement with experimental data on both QY and intrinsic emittance [3].

The importance of including the DoS of the photocathode material (instead of simple approximations for it) in simulation models as well as in the TSM is confirmed by the intrinsic emittance results for Sb, shown in Fig. 4.

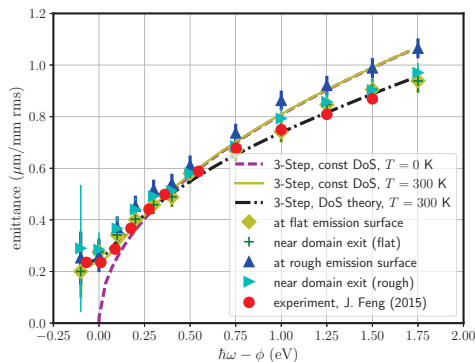


Figure 6: Simulations and 3-step model calculations of intrinsic emittance from Sb are in agreement with experimental data [2] from a flat emission surface only when the antimony DoS and temperature effects are taken into account.

The TSM with the constant DoS over estimates the intrinsic emittance and cannot account for its behavior for $\hbar\omega < \phi$ when the $T = 0$ K Fermi function is used [2, 3]. The results from the simulations with the ridge surface shown in Fig. 6 and in Ref. [3], indicate the emittance growth due to this type of surface roughness.

SUMMARY

Results from simulations and the TSM show the importance of including the DoS of photocathode materials in the modeling in order to obtain agreement with experimental data on QY and intrinsic emittance. The simulations allowed us to investigate the emittance growth due to controlled photocathode surface roughness, effects of finite emission layer thickness and el-el MFPs on quantum yield.

REFERENCES

- [1] J. Feng *et al.*, *Rev. Sc. Instr.*, vol. 86, p. 015103, 2015.
- [2] J. Feng *et al.*, *Appl. Phys. Lett.*, vol. 107, p. 134101, 2015.
- [3] D. A. Dimitrov *et al.*, *J. Appl. Phys.*, vol. 122, p. 165303, 2017.
- [4] K. L. Jensen *et al.*, *J. Appl. Phys.*, vol. 102, p. 074902, 2007.
- [5] C. N. Berglund and W. E. Spicer, *Phys. Rev.* vol. 136, p. A1030, 1964.
- [6] D. H. Dowell *et al.*, *Phys. Rev. ST Accel. Beams*, vol. 9, p. 063502, 2006; D. H. Dowell and J. F. Schmerge, *Phys. Rev. ST Accel. Beams*, vol. 12, p. 074201, 2009.
- [7] W. F. Krolikowski and W. E. Spicer, *Phys. Rev. B*, vol. 1, p. 478, 1970.
- [8] N. E. Christensen and B. O. Seraphin, *Phys. Rev. B*, vol. 4, p. 3321, 1971.